International Journal of Computational Research and Development (IJCRD)
Impact Factor: 5.015, ISSN (Online): 2456 - 3137
(www.dvpublication.com) Volume 4, Issue 1, 2019

CALCULATION OF VISCOUS FLOW AROUND A WING PROFILE USING OPEN FOAM

Raja Ganesh Udayakumar*, Krishnaraj Narayanaswamy* &
Dr. Ing. Habil. Nikolai Kornev**
* M.Sc Student, Computational Science and Engineering, University of Rostock, Germany
** Professor, University of Rostock, Faculty of Mechanical and Marine Engineering,
Chair of Modeling and Simulation, Rostock, Germany

Cite This Article: Raja Ganesh Udayakumar, Krishnaraj Narayanaswamy & Dr. Ing. Habil. Nikolai Kornev, "Calculation of Viscous Flow around a Wing Profile Using Open Foam", International Journal of Computational Research and Development, Volume 4, Issue 1, Page Number 1-9, 2019.

Abstract:

The main intent of this study is to investigate different turbulent models and aerodynamics characteristics of an airfoil. The paper deals with the calculation of viscous flow around a wing profile using OpenFOAM software and a comparison is made between obtained results with the experimental data. The geometry was simplified into a 2D airfoil and the viscous flow field were analyzed at a Reynolds number 3.0×10^6. The chosen airfoil for this experiment is low Reynolds number NREL S809 airfoil. The modelling has been performed in ANSYS 15.0, meshing has been done in ICEM - CFD software and the simulation is performed in OpenFOAM 4.1 software. The main parameters of an airfoil such as coefficients of Lift, Drag, Pressure, and Moment across a range of angle of attacks were calculated using a steady state solver and compared with the experimental data. Comparisons were also done between different turbulence models. Finally the best turbulent model was simulated using an unsteady solver.

Key Words: Computational Fluid Dynamics (CFD), Open FOAM, NREL S809, Airfoil & Aerodynamics

Introduction:

Wind Energy is the most promising renewable energy which has greatly developed in recent years. In past, NACA series airfoils were commonly used for wind turbines but it has some drawbacks. In-order to overcome those drawbacks and the necessity to take wind energy production to next level "NREL" created a set of family of airfoils specially made for horizontal axis wind turbines. The aim of this work is to perform Computational Fluid Dynamics (CFD) simulation for a viscous flow around a two dimensional NREL S809 airfoil using OpenFOAM software. The flow study is done for 4 different models such as k-ε, k-ω SST, Spalart Allmaras and Laminar models. Computation is done for each model with three types of meshes (Coarse, Medium and Fine) and with six different angle of attacks (6 °, 10°, 12°, 14°, 16°, 18°) and a study is made on airfoil parameters. Later the good model is simulated with unsteady or transient solver. For our simulation, k-ε, k-ω SST and Spalart Allmaras Turbulence models were used.

Pre-Processing:

Geometry:

The coordinates for the airfoil S809 were obtained from airfoil plotter tool [13]. The chosen chord length for our study is 2 meters. The airfoil co-ordinates were converted into line body using CATIA V5 software. The line body with ".igs" extension is then imported to ANSYS R 15.0 and a C- Shaped domain with arc diameter 10 meters and a length of 20 meters is created with maximum thickness point of the airfoil as center. The meshing for this geometry is generated using ICEM - CFD tool.

Mesh Generation:

After a study on mesh parameters, structured grid hex mesh is chosen for our geometry because structured meshes are space efficient, they have high resolution and their convergence rate is high when compared with unstructured mesh. The geometry had been divided into 10 blocks with 5 blocks lying very close to the airfoil which has very refined mesh when compared with the remaining blocks which are away from the airfoil. Three mesh refinements were done, namely coarse, medium and fine mesh. The Figure 1 shows the whole mesh of the domain and the refinements near the airfoil for a coarse mesh. Table 1 below shows the number of cells in each meshes and the corresponding YPlus values.

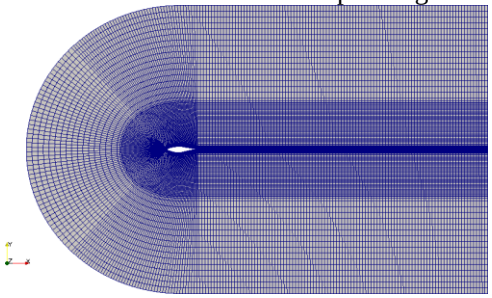

Figure 1: Domain with Coarse Mesh

Table 1: Mesh Information

Mesh Type	No. of Cells	Yplus (Average)
Coarse	23460	240
Medium	79180	160
Fine	197010	90

Computational Methodology:

The *airfoil 2D* case from Open FOAM 4.1 tutorial was taken as a reference and it had been modified according to models. The meshed file with ".msh" extension was imported to Open Foam 4.0 using *fluent3DMeshToFoam* command. The case was initially simulated considering a laminar flow model and later turbulence was turned on in the *turbulence Properties* file with k-ε, k-ω SST and Spalart Allmaras models. These simulations were done using *simple FOAM* solver, which is a Steady-state solver for incompressible flows [2]. Later the model with fine results was solved for unsteady case in *pimple FOAM* solver, which is a transient solver.

Case Setup:

The case setup is done in Open FOAM 4.1 for *Simple FOAM* solver. The corresponding initial conditions were entered for pressure (p), Velocity (U), turbulence kinetic energy (k), specific dissipation rate (ω), turbulence dissipation rate (ε), turbulent viscosity (nut) and kinematic turbulent viscosity (nutilda) in the *0 folder*. The turbulence properties and the transport properties were specified in *constant* folder. The relaxation factors, the residual controls were given in *fv Solution* file. The different schemes used for the simulation mentioned in *fv schemes* file were as follows, *steady State* for time derivative scheme, *Gauss Linear* for gradient scheme. For U, k, ε, ω, nu Tilda the divergence scheme were used alternatively in accordance with the model to get a better converged results. The schemes were *Bounded Gauss linear Upwind V grad (U) bounded Gauss linear Upwind grad (U), bounded Gauss upwind, bounded Gauss limited linear 1.* For the unsteady solver, time derivative scheme was changed as Euler scheme and the remaining were similar as steady state. The above steps were carried out for all the 4 turbulence models with 6 angle of attacks and their corresponding meshes.The velocity for the initial conditions with 6 angle of attacks are tabulated in Table 2. The velocity at each axis is calculated using the formula, Velocity in X-direction = U *cos* (α), velocity in Y-direction = U *sin* (α)

Table 2: Velocity at each axis for 6 angle of attacks

Angle of attack (°)	X-axis (m/s)	Y-axis (m/s)	Z-axis (m/s)
06	22.0783	2.3205	0
10	21.8627	3.8549	0
12	21.7148	4.6156	0
14	21.5405	5.3706	0
16	21.3400	6.1191	0
18	21.1134	6.8601	0

Front face and back face are given as empty for all the parameters.

Post-Processing:

Post processing is done in Open FOAM using Para View which is built in software for post processing. Multiple post processing has been performed like sampling the velocities, pressures, lift coefficients, drag coefficients, moment coefficients of the airfoil S809 for different turbulence models and also for different meshes. These non-dimensional parameters were then compared with the digitized values from [10], Experiment, EllipSys2D, XFoil. *Engauge Digitizer* is used as a digitizer software to take values from [10]. The graph plots were made with the help of *GnuPlot*.

Results and Discussion:

K - Epsilon Model:

The Predicted lift coefficient by the two equation k ε model has satisfactory agreement with the experimental values. From the Figure 2 it can be noted that in the obtained profile, lift goes on increasing till 14° and it starts decreasing after that. In the attached flow region it under predict the lift and over predicts the drag whereas in separate flow region it over predict both lift and drag. Moreover this model fails to predict the stall region, it might be due to inaccurate free stream turbulent intensity value [4]. All the three mesh values follow the same profile in which coarse mesh over predicts the value whereas medium and fine mesh lies near the given values. Since medium mesh results lie very close to the fine mesh results, it can be stated that for this model, number of cells in the medium mesh is sufficient to get the results. The moment coefficient which is shown in Figure 4 follows a profile almost the between Ellipsys2D and X Foil, which is more or less equal to the experimental data but k ε model under predicts the moment coefficient when it gets finer. This might be due to the aerodynamic point. Since we assumed that the point lies at 25% of chord this phenomenon might happened [17]. On taking drag coefficient into account this model over predicts the value. Our obtained drag results from Figure 3 follow the same profile as that of experimental values with over prediction and when we look at the results for different

meshes it seems to be no deviation. In overall values for coefficient of drag differ by huge margin. Even though k ε model might be one of the best model which provide good convergence, it is not suitable for flow with large separation [5] and the above discrepancy in lift and drag coefficients may be due to under prediction of boundary layer [3]. Hence in order to overcome this draw back K ω SST model can be used which is a combination of both k ε and k ω model.

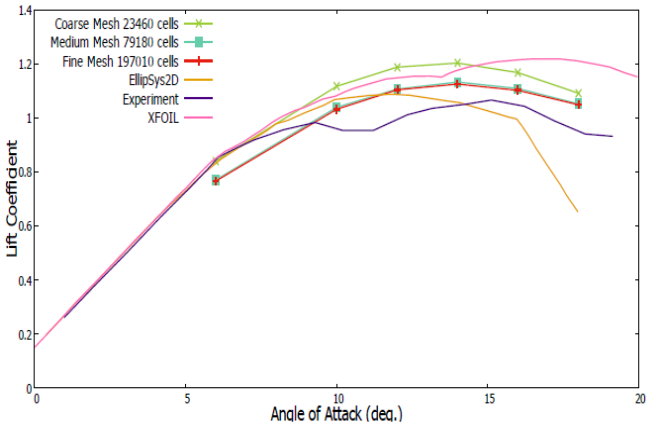

Figure 2: k ε Lift Coefficient curve

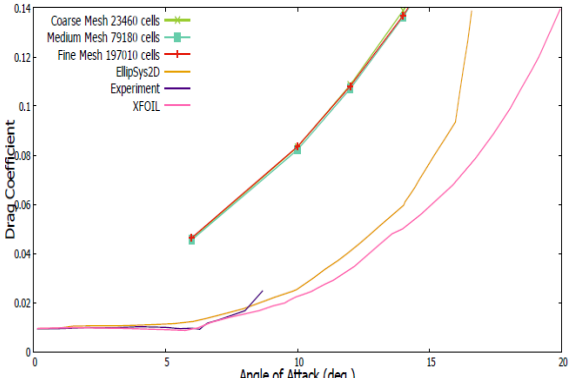

Figure 3: k ε Drag Coefficient curve

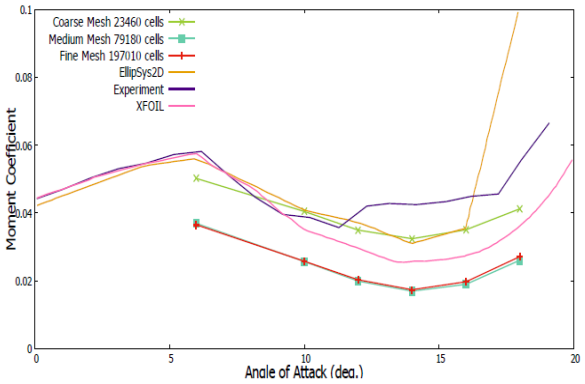

Figure 4: k ε Moment Coefficient curve

K Omega SST Model:

The coarse, fine and medium mesh which were simulated for k ω SST model were compared with the given values from [10]. Most turbulence models have trouble dealing with stall, even if they converge, the results are likely unreliable. Away from walls, the k ω SST model is the same as the standard k epsilon model. In our case, both k ε and k ω SST over predicts the post stall region. When analyzing the mesh qualities, in the pre-stall area fine mesh and medium mesh has almost exact results with that of experiment data and coarse mesh have over prediction. In Post stall region the medium mesh has a good agreement with the experiment.

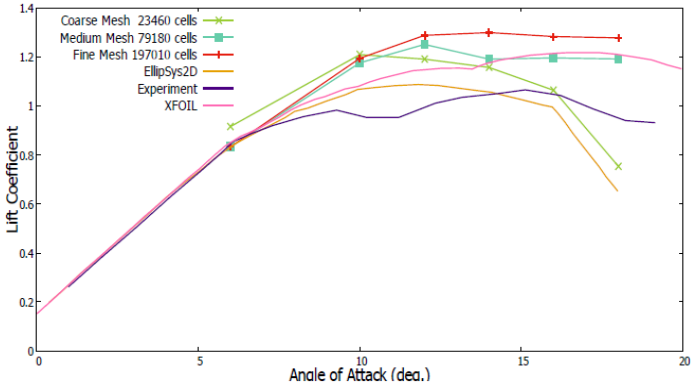

Figure 5: k ω SST Lift Coefficient curve

On comparing the drag coefficient, the results obtained for coarse mesh is slightly over predicted than the results of medium and fine mesh. For both medium and fine mesh the results seems to be in quite agreement with the results of experiment with slight deviation. The Figure 7 describes the moment coefficient versus angle of attack. The moment coefficient was taken by assuming that the aerodynamic center is at one by fourth of the chord [17]. The coarse mesh results are in agreement and the results of fine and medium seems to under predict the values. As it is asymmetric profile moving the aerodynamic center can have a better agreement on the moment coefficient. A detailed discussion were made on this model in upcoming sections.

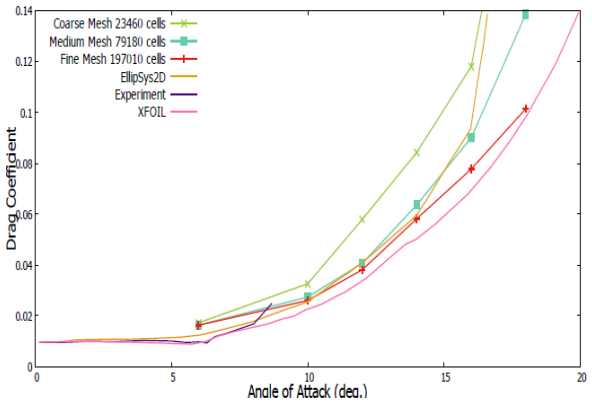

Figure 6: k ω SST Drag Coefficient curve

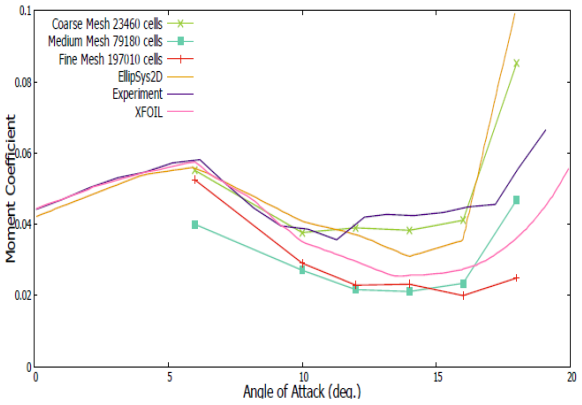

Figure 7: k ω SST Moment Coefficient curve

Spalart Allmaras Model:

The one equation Spalart Allmaras model has satisfactory results for C_l at low angle of attacks and over predicted results for C_d. This model has good agreement with the experimental values for lower angle of attacks. As it can be seen from Figure 8, simulated lift values and experimental lift values are in good agreement till 10°. But after 10°, as the angle of attack increases the values start to vary. Similarly drag coefficient has the same over prediction problem as stated above, whereas moment seems to have good agreement with the given values. Here the turbulence model which is specially designed for aerodynamics calculations fails to predict the values exactly and it may be due to the usage of wall functions [6]. This model gives the good results when the resolution is very high, the Yplus value should be in the Viscous sub layer (YPlus < 5), but here we have used the wall function as our Yplus value lies in the logarithmic region (Yplus>30). Another reason for the over prediction may be due to the fact that Spalart Allmaras model does not perform well in the region where flow starts to separate [14].

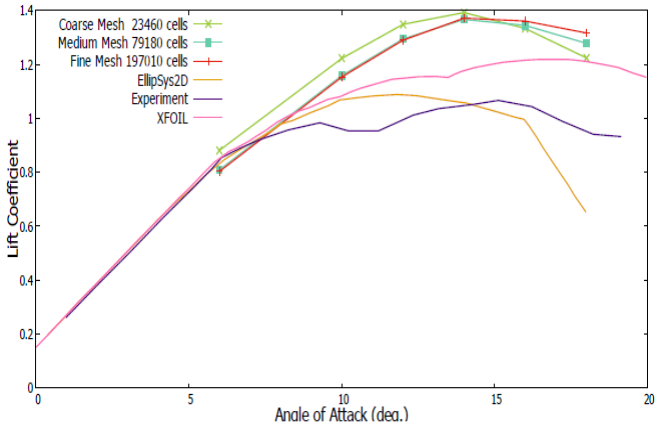

Figure 8: Spalart Allmaras Lift Coefficient curve

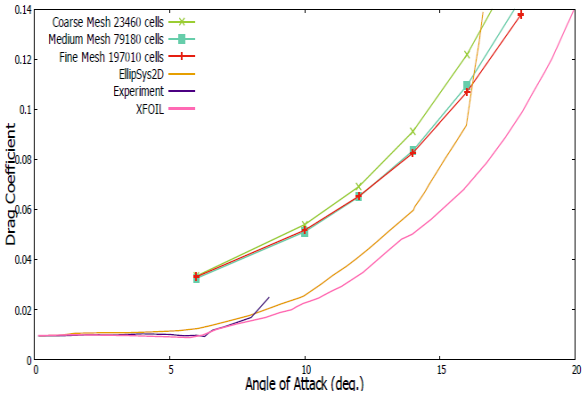

Figure 9: Spalart Allmaras Drag Coefficient curve

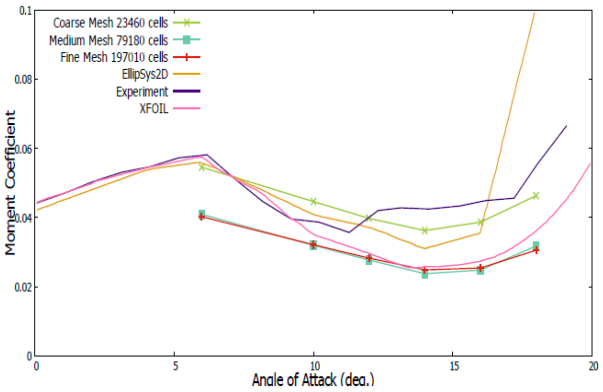

Figure 10: Spalart Allmaras Moment Coefficient curve

Detailed Discussion about the Best Model:

The flow analysis around the airfoil S809 using the different turbulent models were compared and it's illustrated in this chapter. The experimental data show that at a positive angle of attack approximately below 5°, the flow remains laminar over the forward half of the airfoil. It then undergoes laminar separation followed by a turbulent reattachment. As the angle of attack increases further, the upper-surface transition point moves forward and the airfoil begins to experience small amounts of turbulent trailing edge separation. At approximately 9° almost 5% to 10% of the upper surface is separated from the flow. The upper-surface transition point has moved forward approx. towards the leading edge. As the angle of attack is increased to 15°, the separated region moves forward to the mid of the chord. Further increase in angle of attack, the separation moves rapidly forward to the vicinity of the leading edge, so that at about 20°, most of the upper surface is stalled (deep stall) [7] .The results of fine meshed domain of all the turbulent models are presented as graphs which are compared with Experiment, EllipSys2D, XFoil and they are shown in Figures 11, 12, 13.

From the Coefficient of lift graph it can be seen that lift for the k - ε model and k - ω SST model lies close to the experimental values for the initial smaller angle of attacks. In k - ε model the attached flow region under predicts the lift and over predicts the drag whereas in separate flow region it over predicts both lift and drag. This model fails to give results for drag and also fails to predict stall angle, this may occur in k-ε model because it has discrepancy in predicting the adverse pressure gradient and boundary layer [3]. On the other hand the k - ω SST model which shows good agreement with adverse pressure region and it shows almost acceptable results for Coefficient of drag. In higher angle of attacks there is a considerable over prediction in the lift for this model which is due to the turbulence levels in the boundary layer which were high. This leads to delay the separation so that the pressure in the suction side spreads over more area of the airfoil which leads to increase in lift. In general the k-ω SST model will over predicts the lift coefficient beyond the stall point [9].

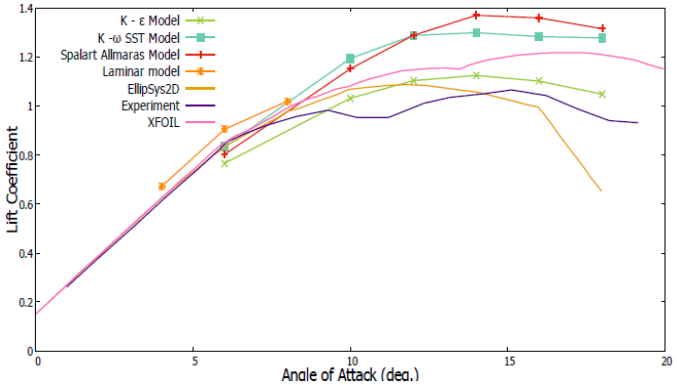

Figure 11: Lift Coefficient comparison curve for fine mesh

On comparing the coefficient of moment for both k ε model and k ω SST model, both shows a better agreement with the XFoil results. The aerodynamic center is responsible for the coefficient of moment. In our cases we had assumed the aerodynamic center to be 25% of chord length [17] so we had satisfactory values of Coefficient of moment.

On taking Spallart Allmaras model in to account, this model also has a good agreement with the

experimental values for lower angle of attacks but for higher angle of attack it over predicts the values and the drag coefficient seems to be not in range with the experimental value this may be due to the use of wall functions as stated above in the previous section.

On taking laminar model into account, in general maintaining a laminar boundary layer in an airfoil will minimize the drag which leads to increase in efficiency, but maintaining laminar flow in real world is messy. According to the experimental study the flow remains Laminar over the forward half of the airfoil [1]. In our simulation, for lower angle of attack (less than 6°) the airfoil has a favorable pressure gradient which makes laminar flow possible and the results are quite agreement with the experimental value with a small over prediction. When angle of attack increases the flow separation gets increased and there exist an adverse pressure gradient. So it's impossible to get a converged solution for higher angle of attacks using laminar model. For a laminar flow the favorable pressure gradient ends somewhere in between 30% to 75% of chord [15]. On simulating laminar model, we could not get a converged solution for

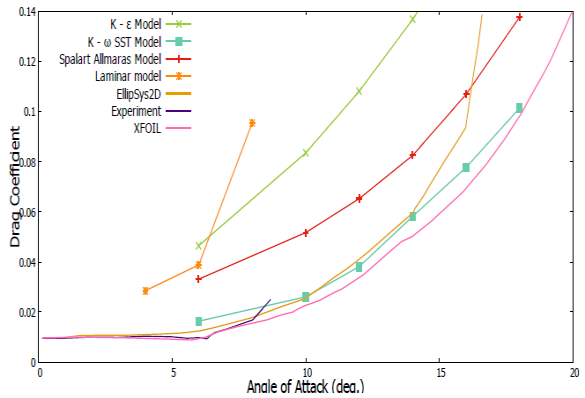

Figure 12: Drag Coefficient comparison curve for fine mesh

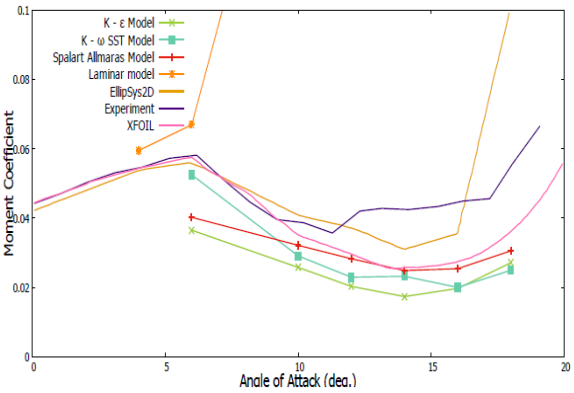

Figure 13: Moment Coefficient comparison curve for fine mesh

higher angle of attacks. On comparing all the models it is evident that the k ω SST model has the C_l, C_d and C_m values close to the given experimental values which can be confirmed using the Table 3, which clearly shows that k ω SST model has the lowest error than other models.

Table 3: Error difference for 6° Angle of attack

Model	C_d	% error in C_d	C_l	% error in C_l
K Omega SST	0.016375	36.5	0.834075	1.51
K Epsilon	0.046527	287.7	0.766789	9.46
Spalart Allmaras	0.033143	176.2	0.803366	5.16

This can be even studied closer using the stream lines and pressure coefficient graphs which are described below.

Streamline:

Streamlines are used to trace the direction of flow at particular location or through the whole domain. Here we can see the streamlines of flow at 6.0° and 18.0° angle of attack with different color gradient which shows the velocity distribution of the flow. Through streamline the wake region development can also be studied clearly. In the Figure 14(a) the wake region is smaller than Figure 14(b). This development is due to separation of flow which gets changed when angle of attack is increased.

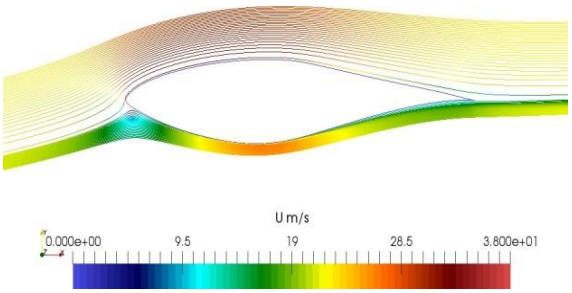

(a) α=6.0°

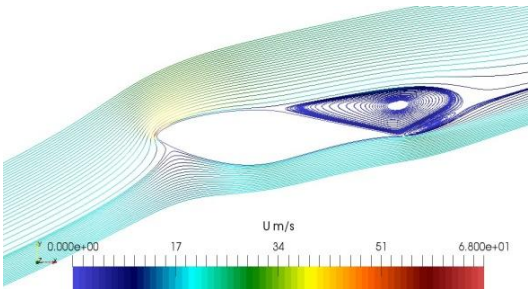

(b) α =18.0°

Figure 14: Streamline

Pressure Coefficient Graphs:

The pressure coefficient for the fine mesh k ω SST model was compared with the Ellip Sys 2D and XFoil values which are shown in the following Figure 15 for 6.0° and 18.0° angle of attack. The pressure obtained from OpenFOAM is a pressure distribution values from which the non-dimensional coefficient of pressure is calculated by sampling in ParaView. The pressure coefficient describes the relative pressure through- out the flow. From the figures it is evident that the low pressure area in the upper surface of the foil tends to expand when the angle of attack increases. The profile we obtained, follows the traces of XFoil results which shows that our k ω SST model results are in good agreement with the given values.

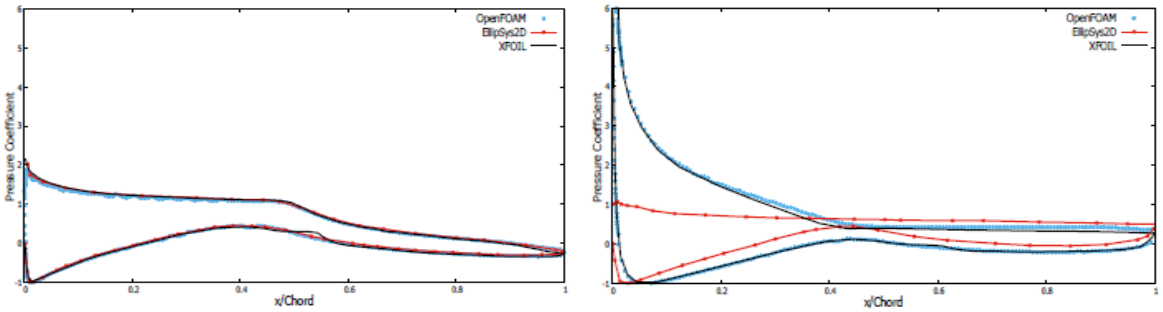

(a) α=6.0° (b) α =18.0°

Figure 15: Pressure Coefficient graph for K ω SST model fine mesh

Skin Friction Coefficient Graphs:

In our case the Open Foam gives the value of wall shear stress with the help of the command *simple Foam post Process –func wall Shear Stress* and then the shear stress is mapped in para View and the skin friction Coefficient is calculated on the surface of airfoil using calculator option.

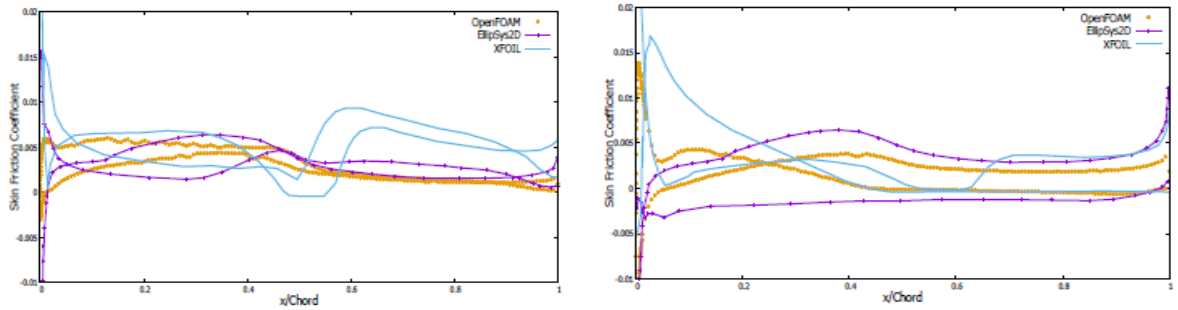

(a) α = 6.0° (b) α =18.0°

Figure 16: Skin Friction Coefficient graph for K ω SST model fine mesh

The computed skin friction Coefficient for the fine domain of k Omega SST for different angle of attack is compared with the Ellipsys2D and XFoil values. The obtained results for k ω *SST* gets the profile which is approximately similar to the path trajectory of the XFoil. The wall shear stress developed in the upper surface at leading edge after stagnation point gets increased when the angle of attack increases. This leads to growth of skin friction coefficient at the leading edge. In the trailing edge there is a significant increase in the skin friction coefficient. This is because of the shear created by the flow which leaves the trailing edge. The Figure 16 shows the skin fiction coefficient for different angle of attack.

Velocity Distribution:

Velocity distribution profile for k ω SST model at 6.0° & 18.0° angle of attack are shown in Figure 17. Our profile follows the typical velocity distribution. As stated already velocity is zero at the stagnation point on the leading edge and then on the suction side of the airfoil the velocity is high whereas velocity will be low in the pressure side of the airfoil. The flow separation gets increased as the angle of attack is increased. This increase of flow separation will results in increase of wake region. The flow separation for different angle of attacks can be clearly seen in the figures, where 6.0° angle of attack has small separation and small wake region whereas 18.0° has high separation and larger wake region. The velocity inside the wake region will below.

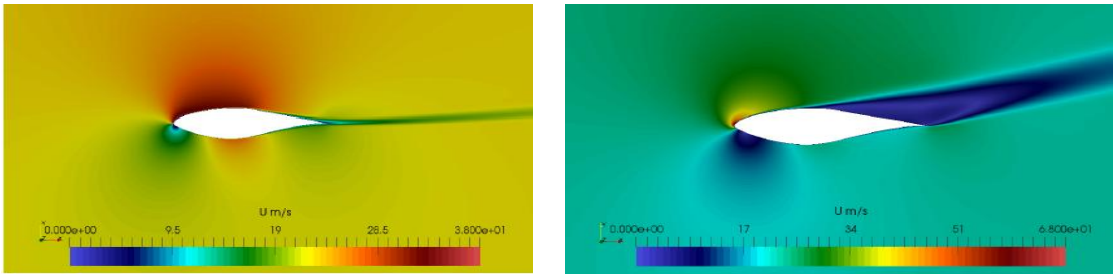

(a) α=6.0° (b) α =18.0°

Figure 17: Velocity Distribution for each 6.0° and18.0°angle of attack

Pressure Distribution:

High pressure will be created on the stagnation point as the velocity there will be zero. The pressure distribution in the pressure side of the airfoil will be more when compared with the pressure on the suction side of the airfoil, which will be less.

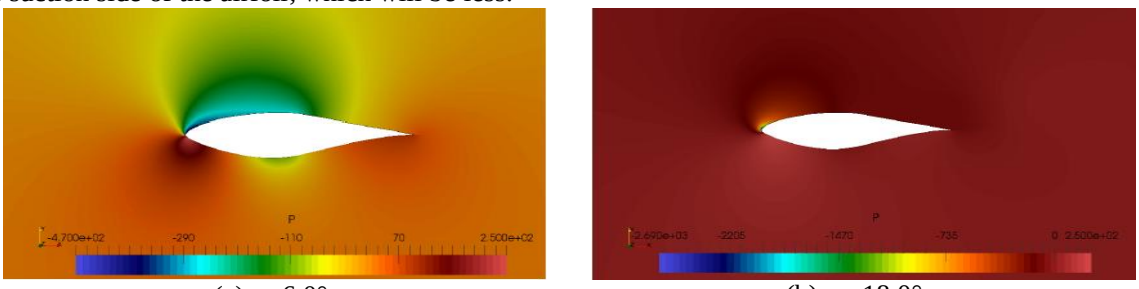

(a) α=6.0° (b) α =18.0°

Figure 18: Pressure Distribution for each angle of attack

Unsteady Case:

The unsteady case in our airfoil is done with pimple Foam solver which is a transient solver. The flow properties changes with respect to space and time. Since k ω SST model shows better results, this transient simulation was carried out for the k ω SST model with a fine mesh domain. In our case the flow was made to pass through the entire domain nearly 5 times, so the averaged time interval is approx 5 seconds and the plots were done for lift, drag, moment coefficients versus the averaged time period.

For lower angle of attack the C_l, Cd and C_m tends to attain a stabilized value corresponding to the steady state results. As the angle of attack increases the values of C_l, C_d and C_m has a higher amplitude for initial time step and the *crest* and *trough* has attained lower amplitude throughout the entire period of time. This phenomena is because of the unsteady nature of the flow and also the flow separation and reattachment which occurs simultaneously correspondence with time.

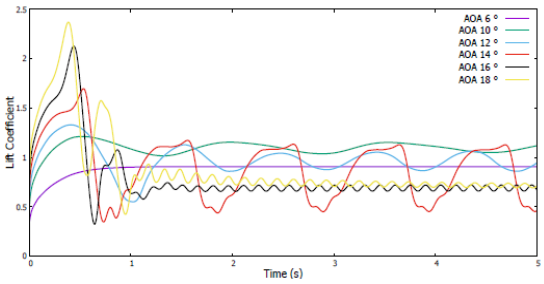

Figure 19: Unsteady case Lift Coefficient

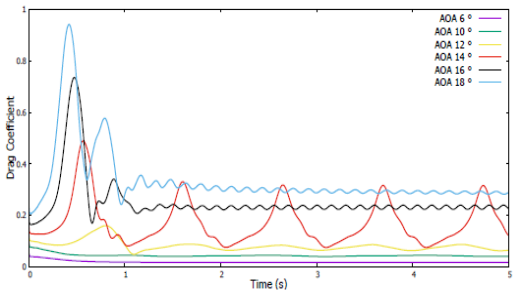

Figure 20: Unsteady case Drag Coefficient curve

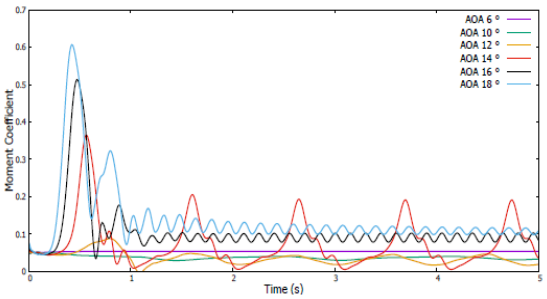

Figure 21: Unsteady case Moment Coefficient curve

The Figure 22 shows the axial velocity distribution at different x/c in the far field region for 6.0° angle of attack in an unsteady flow. At the trailing edge (x/c = 1) there is a sudden fall in velocity which shows separation of flow (wake region). As the plot moves further one can see the velocity drop gets decreased which tends to attain uniformity. This is due to the flow reattachment in the far field.

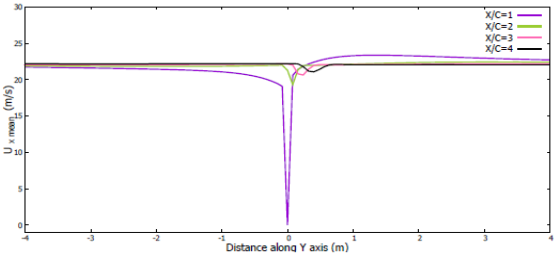

Figure 22: Axial velocity

Conclusion:

Two dimensional viscous flow analysis around a wind turbine airfoil NREL S809 was performed using Open FOAM software. The analysis was carried out using 4 different models for a Reynolds number 3.0×10^6. From the above simulations k ε and Spalart Allmaras model gave near prediction to the experimental values at low angle of attacks whereas k ω SST model gives very close prediction in both pre stall and post stall regions. k ε model can be considered as good model for this airfoil but while taking drag into account k ε model over predicts the C_d values whereas C_d value of k ω SST model lies close to the experimental values. Furthermore the behavior of the k ω SST model in the logarithmic region is superior to that of the k ε model in adverse pressure gradient flows [8]. Hence, it is concluded that from the simulated 4 different turbulent models K ω SST model is satisfactory.

The obtained results of K ω SST model can increased further by, reducing the Reynolds number (as S809 is a low Reynolds number airfoil made for $Re \leq 2\times10^6$) [1, 4] or by reducing the modelling and discretization errors, because here the airfoil was fixed and flow direction was changed for every angle of attacks which may cause an error due to fixed meshing. Designing separate domain models for each angle of attack may circumvent this error, or it can also be improved by limiting the eddy viscosity from the buffer zone to log zone using a continuous damping function so that the results almost matches with the experimental values (as presented in World Energy Renewable congress 2011, Sweden) [11], or also by avoiding the wall functions and by having a very fine resolution of the mesh, better results can be obtained [16].

References:

1. Dan M. Somers, Design and Experimental Results for the S809 Airfoil, NREL, January 1997.
2. Christopher J. Greenshields, CFD Direct Ltd, OpenFOAM User Guide 5.0, Open- Foam Foundation Ltd, July 2017.
3. David Hartwanger and Dr Andrej Horvat, 3D Modelling of a Wind Turbine Using CFD, UK Conference, 2008.
4. Ouahiba Guerri Khadidja Bouhadef and Ameziane Harhad Turbulent Flow Simulation of the NREL S809 Airfoil, Wind Engineering Volume 30, No. 4, 2006.
5. T. S. D. Karthik, Turbulence Models and their Applications, Department of Mechanical Engineering, IIT Madras, 2011.
6. Fernando Joel Lopes Gamboa, Numerical Analysis of a Wing Sail Aerodynamic Characteristics Using Computational Fluid Dy- Namics - PART I, IST, 2010.
7. Walter P. Wolfe, Stuart S. Ochs, CFD Calculations of S809 Aerodynamic Characteristics, AIAA-97- 0973.
8. Avi. H. C, Madhukeshwara. N, S. Kumarappa Numerical Investigation of Flow Transition for NACA – 44
9. P. Catalano and M. Amato, An evaluation of RANS turbulence modeling for aero- dynamics, Aerospace Science and Technology 7, 2003, pp. 493-509
10. Bertagnolio, F., Sørensen, N. N., Johansen, J., and Fuglsang, P. (2001). Wind turbine airfoil catalogue. (Denmark. Forsknings center Risoe. Risoe-R; No. 1280 (EN)).
11. Tawit Chitsomboon, Chalothorn Thamthae, Adjustment of k ω SST turbulence model for an improved prediction of stalls on wind turbine blades, World Renewable Energy Congress Sweden, 2011.
12. https://www.comsol.de/multiphysics/mesh-refinement
13. http://airfoiltools.com/airfoil/details?airfoil=s809-nr
14. http://www.engineering.com/designsoftware/designsoftwarearticles/articleid/13743/choosing-the right-turbulence-model-for-your-cfd-simulation.aspx
15. http://www.aviation-history.com/theory/lam-flow.html
16. https://turbmodels.larc.nasa.gov/sst.html
17. https://en.wikipedia.org/wiki/aerodynamic_center